Plasma Medicine, 5(2–4): 189–203 (2015)

Study of the Power Distribution of Each Impedance in the Electrical Circuit of Ionized Gas Coagulation Equipment

Hajime Sakakita,[1,2,*] Satoru Kiyama,[1] Jaeho Kim,[1] Hiromasa Yamada,[1,2] Isao Masukane,[1] Toru Niwa,[3] Nobuyuki Shimizu,[4] Yasuyuki Seto,[5] Masao Ichinose,[3] & Yuzuru Ikehara[1,6]

[1]Innovative Plasma Processing Group, Electronics and Photonics Research Institute, National Institute of Advanced Industrial Science and Technology (AIST), Tsukuba Central 2, 1-1-1 Umezono, Tsukuba, Ibaraki 305-8568, Japan; [2]Department of Engineering Mechanics and Energy, Graduate School of Systems and Information Engineering, the University of Tsukuba, 1-1-1 Tennoudai, Tsukuba, Ibaraki 305-8573, Japan; [3]Wakayama Medical University, 811-1 Kimiidera, Wakayama, Wakayama 641-8509, Japan; [4]SANNO Hospital, International University of Health and Welfare, 8-10-16 Akasaka, Minato, Tokyo 107-0052, Japan; [5]Department of Gastrointestinal Surgery, The University of Tokyo Hospital, 7-3-1 Hongo, Bunkyo, Tokyo 113-8655, Japan; [6]Biotherapeutic Research Group, Biotechnology Research Institute for Drug Discovery (AIST), Tsukuba Central 5, 1-1-1 Higashi, Tsukuba, Ibaraki 305-8565, Japan; E-mail: h.sakakita@aist.go.jp

*Address all correspondence to: Hajime Sakakita, National Institute of Advanced Industrial Science and Technology, Tsukuba Central 2, 1-1-1 Unezono, Tsukuba, Ibaraki 305-8568, Japan; Tel.: +81298615775; Fax: +81298615149; h.sakakita@aist.go.jp

ABSTRACT: Medical plasma equipment is categorized as electrical equipment for use in medical treatment. The characteristics of both low-energy ionized gas coagulation equipment (LE-IGCE) as a low-temperature plasma source and high-energy ionized gas coagulation equipment (HE-IGCE) as a high-temperature plasma source strongly depend on the structure of the plasma equipment and the operating conditions. In this paper, to ensure the electrical safety of both the LE-IGCE and the HE-IGCE, the output current and power of both types of equipment are measured, and the power distribution is evaluated for each impedance in the electrical circuit. The power required to produce plasma using the LE-IGCE corresponds to the real power of the power supply, and it is higher than that required by the HE-IGCE. However, ohmic heating in the human body caused by the LE-IGCE is much lower than that caused by the HE-IGCE.

KEY WORDS: plasma flare current, load power, blood coagulation, cauterization, minimally invasive surgery, low temperature plasma, high temperature plasma, International Electronics Commission

I. INTRODUCTION

A. Clinical Need for Medical Plasma Equipment for Progress in Minimally Invasive Surgical Procedures

Abdominal surgery is commonly carried out on patients with diseases of either the digestive tract or the female reproductive system. Minimal surgical invasiveness is one of the ideal conditions for such operations that surgeons strive to achieve. Surgeons

1947-5764/15/$35.00

conventionally control bleeding using methods such as cauterization, clipping, or ligation, depending on the types of blood vessel encountered during omentectomy. Stopping bleeding with a high-frequency electrical coagulator (HFEC) is based on the destructive obstruction of the blood vessel, and it causes prolonged postoperative disorder and scar tissue formation in the abdominal cavity. Consequently, HFEC should not be used on the brain or the heart. Almost all surgeons have encountered latent problems caused by thermal effects, such as burn injuries. During an excision, burned out scars were produced when using high-frequency electrical currents. These scars are possible causes of adhesion and ileus after operations. In surgical procedures, the equipment that reduces tissue damage and offers controllability is urgently required. Plasma energy, which is produced by equipment that is intended for thermal coagulation of tissues, has been used in practice in an endoscopic submucosal dissection (ESD), the ablation of residual tumor cells, and to control bleeding.[1] In principle, however, this system produces currents against the human body and causes arc discharges. The limited treatment times available do not completely stop the bleeding or ablate residual tumors. This is not an effective way to use the plasma energy. During ESD treatment, the perforation risk is generally higher when using this type of plasma coagulator rather than the HFEC. Therefore, the HFEC has advantages when stopping bleeding. Glow-like plasma, which does not produce arc discharges in principle, is suitable for applications where it is necessary to reduce tissue damage while sufficiently coagulating the blood. Burn injuries caused by cauterization when used to control bleeding is another major issue. The scar tissue that results from such burn injuries is characterized as a proliferation of fibroblast and blood vessels, called granulation tissue, which limits the adaptability of the method to laparoscopic surgery and the ability to perform a second surgery, as shown in Fig. 1.

B. Equipment to Control Bleeding from Small and Capillary Vessels

Clipping, ligation, or cauterization are used as the basic methods to control bleeding from small or mid-sized arteries. For the control of bleeding from small and capillary vessels, HFEC, ultrasonic wave equipment, laser, and high-temperature plasma are commonly used. Operating points for hemostasis can be classified into two categories: with or without cauterization. Low-temperature plasma directly accelerates the blood coagulation process, whereas the other methods essentially cauterize the capillaries, small vessels, and veins using heat, ultrasonic vibration, and high-frequency current-based heating, as summarized in Fig. 2. From the viewpoint of prioritizing medical electrical equipment safety, these two types of high- and low-temperature plasma equipment have not yet been defined by the specifications of the International Electronics Commission (IEC). However, high-temperature plasma is partially categorized in IEC 60601-2-2 (particular requirement for high frequency surgical equipment).[2]

Here, we introduce an example of low-energy ionized gas coagulation equipment (LE-IGCE) using a low-temperature plasma. In general, plasma, which is defined as ionized gas, is composed of charged particles (i.e., ions and electrons) that have been ionized from atoms or molecules, and excited particles. The main examples of high-

FIG. 1: Photograph taken just before second surgery in the University of Tokyo Hospital. It is difficult to locate the area upon which the operation is to be performed, because of the tissue adhesion caused by the HFEC operation at first surgery

temperature plasmas include the sun, auroras, lightning, nuclear fusion plasma, and plasma sprays. Low-temperature plasmas have been adopted in the manufacturing of semiconductors, thin-film solar panels, single crystal diamonds, and fluorescent lamps. Recently, low-temperature atmospheric pressure plasmas have been produced by several methods.[3–8] Plasma technologies are already used in medical applications, such as to coat a stent with diamond-like carbon and to modify biomaterials.

The LE-IGCE for blood coagulation comprises a control unit, a gas feed line, a power source, and the plasma source.[9–15] A "plasma flare" produced by this plasma source has been applied to bleeding body parts after excision of the femoral artery under anesthesia.[13,14] Here, a plasma flare is defined as visible light passing from the equipment to the target. Coagulation is promptly induced, covering the disrupted blood vessel and stopping the bleeding. The surface temperature during this treatment is less than 40°C.[14] There is no evidence that the heat generated by this process causes burns or tissue damage. Plasma treatments can thus reduce invasiveness during hemostasis, and reduce the risk of postoperative disorders.

	Without cauterization	Cauterization generally occurs			
	Low-temperature plasma	**High-temperature plasma**	**Laser**	**Ultrasonic wave equipment**	**High-frequency electrical coagulator**
Operating points for hemostasis	Acceleration of blood coagulation process	Heating to destroy small blood vessel	Heating to destroy small blood vessel	Ultrasonic vibration and heating to destroy small blood vessel	High frequency current heating to destroy small blood vessel
Adaptation for bleeding control	Capillaries, small vessels, and veins	Capillaries, small vessels, and veins	Capillaries, small vessels, and veins	Capillaries, small vessels, and veins	Capillaries, small vessels, and veins
Measurement of output parameter	**Not defined**	△	○	○	○

FIG. 2: Summary of categories of operations used to stop bleeding for capillaries, small vessels and veins, with or without cauterization. The basic safety of the low temperature plasma is not defined by IEC specifications

High-energy ionized gas coagulation equipment (HE-IGCE) has been used effectively as a high-temperature plasma source in surgical procedures.[1] With the realization of low-temperature and highly-reactive atmospheric-pressure plasma that can stop bleeding, minimally invasive operations are expected to become the norm in the near future. Realization of international standards for the basic performance and safety of medical plasma equipment for blood coagulation applications must therefore accelerate to extend the possibilities of use of such equipment. The characteristics of LE-IGCE and HE-IGCE are strongly dependent on the structure of the plasma equipment and the operating conditions. Therefore, to apply these plasma sources effectively, safely, and reproducibly, it is necessary to clarify the correlation parameters between the plasma components and the biological effects of the plasma. To ensure the safety of the LE-IGCE, specifications such as the output current and power of the equipment must be measured and evaluated.[16,17]

II. EXPERIMENTAL SETUPS FOR REAL TIME CURRENT MEASUREMENT OF THE PLASMA FLARE

At a minimum, the following must be defined to establish new specifications: (1) testing methods for the electrical characteristics of medical plasma equipment, (2) testing procedures, (3) measurement systems, and (4) test criteria. Many components of ionized

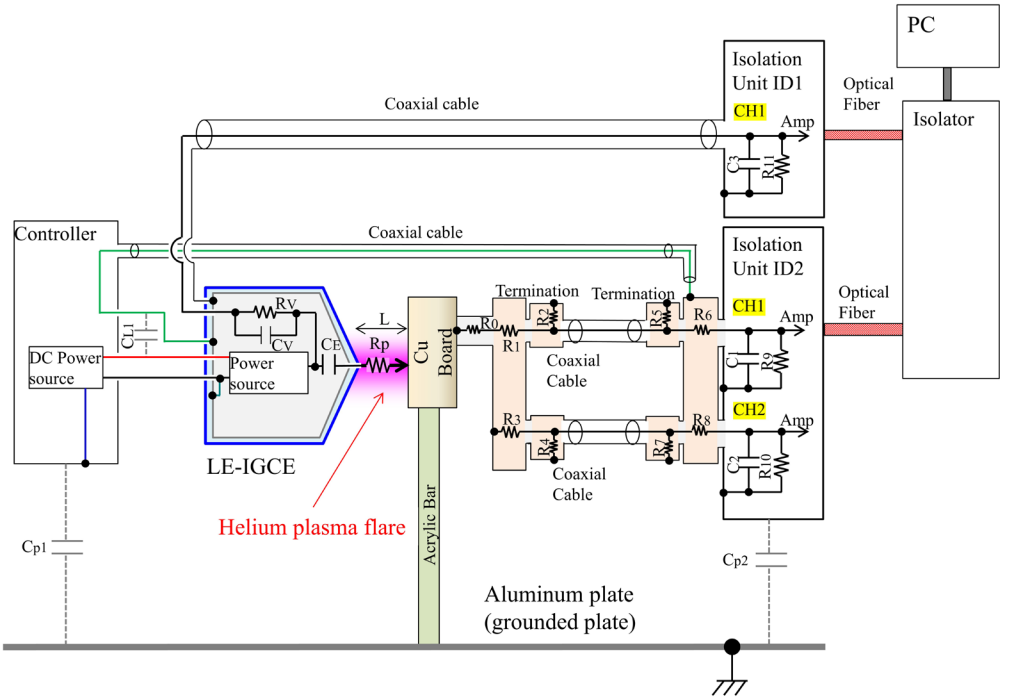

FIG. 3: Schematic diagram of the electrical circuit used to measure the real-time current and voltage for the LE-IGCE

gas coagulation equipment are not fully covered by IEC 60601-1 (General requirements for basic safety and essential performance),[18] IEC 60601-1-2 (EMC),[19] IEC 60601-2-2,[2] and ISO 14971 (Risk management).[20] Alpha rays, beta rays, gamma rays, microwaves, ultraviolet rays, visible light, and infrared rays are not defined in the IEC standards, except for lasers and light-emitting diodes. The plasma flare might be categorized as visible light.

A real-time plasma current measurement system for plasma flare characteristics measurement that uses a resistance is illustrated in Figs. 3 and 4. A plasma flare is used to treat a target material composed of a copper plate, which is supported by an insulated stand. A current is circulated through the resistance unit (RU). The signals are stored in a floating analog–digital converter. Here, DM-8000 and DM900 series by Iwatsu Instruments Corporation were used. In the case of helium plasma flare current measurement for the LE-IGCE, each resistance and capacitance of the RU shown in Fig. 3 are set as follows: R_0 = 1 kΩ, Rp ~1 MΩ, R1 = 50 Ω, R2 = 50 Ω, R3 = 50 Ω, R4 = 50 Ω, R5 = 50 Ω, R6 = 50 Ω, R7 = 50 Ω, R8 = 50 Ω, R9 = 1 MΩ, R10 = 1 MΩ, Cp1 = 1,000 pF, Cp2 = 500 pF, CL1 = 500 pF, CE = 2 pF, C1 = 20 pF, C2 = 20 pF, C_3 = 1122 pF, C_V = 5.5 pF, R_V = 204 MΩ, and R_{11} = 1 MΩ. In this article, minimally invasive plasma equipment was used as the LE-IGCE.[14,21,22]

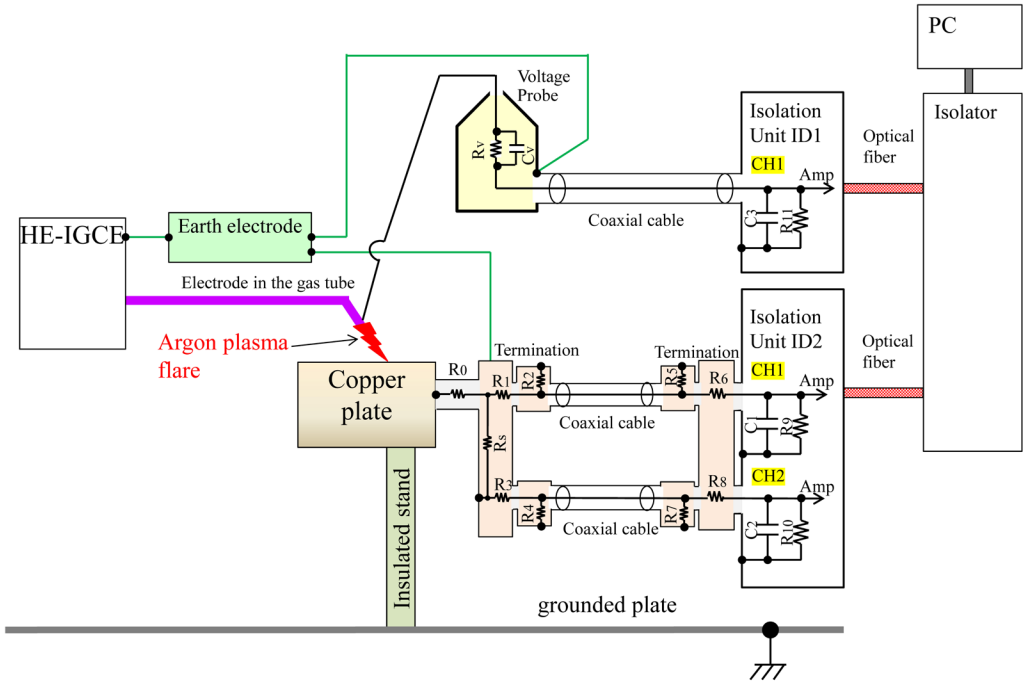

FIG. 4: Schematic diagram of the electrical circuit used to measure the real-time current and voltage for the HE-IGCE

In the case of argon plasma flare current measurement of the HE-IGCE, each resistance and capacitance of the RU shown in Fig. 4 are set as follows: R_0 = 4 kΩ, R1 = 50 Ω, R2 = 50 Ω, R3 = 50 Ω, R4 = 50 Ω, R5 = 50 Ω, R6 = 50 Ω, R7 = 50 Ω, R8 = 50 Ω, R9 = 1 MΩ, R10 = 1 MΩ, R11 = 1 MΩ, RS = 50 Ω, C1 = 20 pF, C2 = 20 pF, C3 = 15 pF, C_V = 3 pF, and R_V = 100 MΩ. In this article, the VIO APC 2 system by ERBE Elektromedizin GmbH was used as the HE-IGCE.[1,22,23]

III. EXPERIMENTAL RESULTS AND DISCUSSION

As one method used to evaluate the characteristics of plasma flares, the time variations of the high voltage (secondary voltage) applied to the electrode and the helium plasma flare current flowing to the target plate have been measured, as shown in Fig. 5(a). The helium gas, with purity of 99.995%, flowed at a rate of 2.0 L/mm. In the case of a primary voltage of 18 V DC and a distance (L) of 10 mm between the exit of the plasma equipment and the target, the time variations of both voltage and current are measured with 10 ns sampling times. Here, R_0 = 1 kΩ is used as the load resistance. A high voltage sinusoidal waveform with frequency of ~60 kHz is applied. During the positive voltage period, positive ions flow into the target plate. In contrast, during the negative voltage period, electrons flow into the target plate. During these periods, the plasma flare

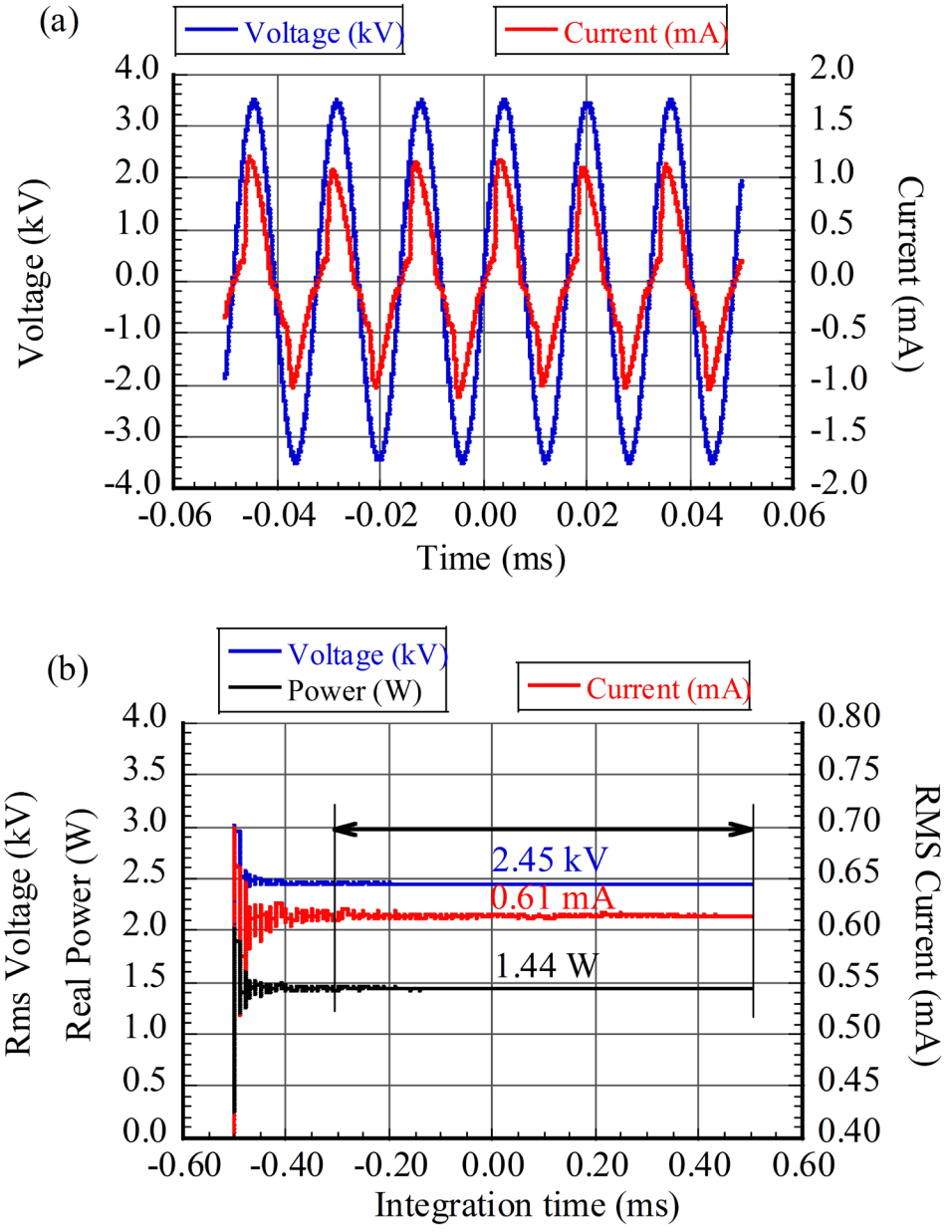

FIG. 5: (a) Time evolutions of the high voltage and the current applied by the electrode through the target plate, and (b) time-integrated voltage, current and power characteristics, which are RMS voltage, RMS current, and real power, respectively

is produced between the exit of the plasma equipment and the target; this was already confirmed by Fujiwara et al.[24] Figure 5(b) shows the root mean square (RMS) voltage, the RMS current, and the real power as functions of the integration time, and these pa-

rameters are calculated using equations (1), (2), and (3), respectively.

$$(1)\quad V(t) = \sqrt{\frac{1}{t}\sum v(t)^2 \times \Delta t}$$

$$(2)\quad I(t) = \sqrt{\frac{1}{T}\sum i(t)^2 \times \Delta t}$$

$$(3)\quad P(t) = \frac{\sum v(t) \cdot i(t) \cdot \Delta t}{t}$$

Here, *V(t)* is the RMS voltage, *I(t)* is the RMS current, *P(t)* is the real power, *t* is time, *v(t)* is the measured voltage, *i(t)* is the measured current, Δt is the sampling time, T =Δt x (n + 1), and *n* represents the number of data points. To calculate the real power, *v(t)* and *i(t)* are multiplied, and the integrated integral is determined using 1 ms (100,000 samples) of data. The data are averaged using 80,000 samples (final period of 0.8 ms), as indicated in Fig. 5(b).

Fig. 6 shows the RMS voltage, the RMS current, and the real power as a function of distance, *L*. The RMS voltage decreases as L decreases, whereas the RMS current increases sharply as *L* decreases. The real power increases slightly as *L* decreases. In this case, the voltage was not controlled to maintain constant power for each *L*.

Fig. 7 shows a schematic diagram of the electric circuit for study of the power distribution for each impedance of the LE-IGCE. In the case where C_C = 2 pF and the operating voltage frequency f = 60 kHz, then the impedance becomes 1.33 MΩ. The equivalent resistance for the human body R_L is 1 kΩ, and the resistance for the leakage current measurement R_M is 200 Ω, as defined by the IEC specification.[2,18] The plasma resistance, R_p, is assumed to be 1.5 MΩ, and then R_L and R_M are negligible. Here, V_{peak} = 4 kV, ω = 2πf is selected, and then the RMS current, $I_{P\text{-}RMS}$, is calculated to be 1.41 mA using equation (4). This estimated value is very close to the measured value shown in Fig. 6.

$$(4)\quad I_{p\,RMS} = \frac{V_{peak}}{\sqrt{2}R_p}\frac{\omega C_c R_p}{\sqrt{1+\omega^2 C_c^2 R_p^2}}$$

The real power of the plasma, P_r, is calculated as follows:

$$(5)\quad P_r = I_{PRMS}^2 \times R_P = (1.41 \times 10^{-3})^2 \times 1.5 \times 10^6 = 3.0\,W$$

P_r corresponds to nearly the average real power of the power supply, because the other additional power components are comparatively very small, as described later. The voltage and the power of the equivalent resistance for the human body are calculated to be 1.4 V (1 kΩ × 1.4 mA), and 2 mW [1 kΩ × (1.4 mA)^2], respectively. The power of the resistance used for the leakage current measurements is calculated to be 400 μW. Therefore, the ohmic heating of the plasma flare current is negligible in the human body, but a part of the energy that is used to produce the plasma flows into the human body. As an example, a helium plasma flare was used to treat the bleeding that was induced

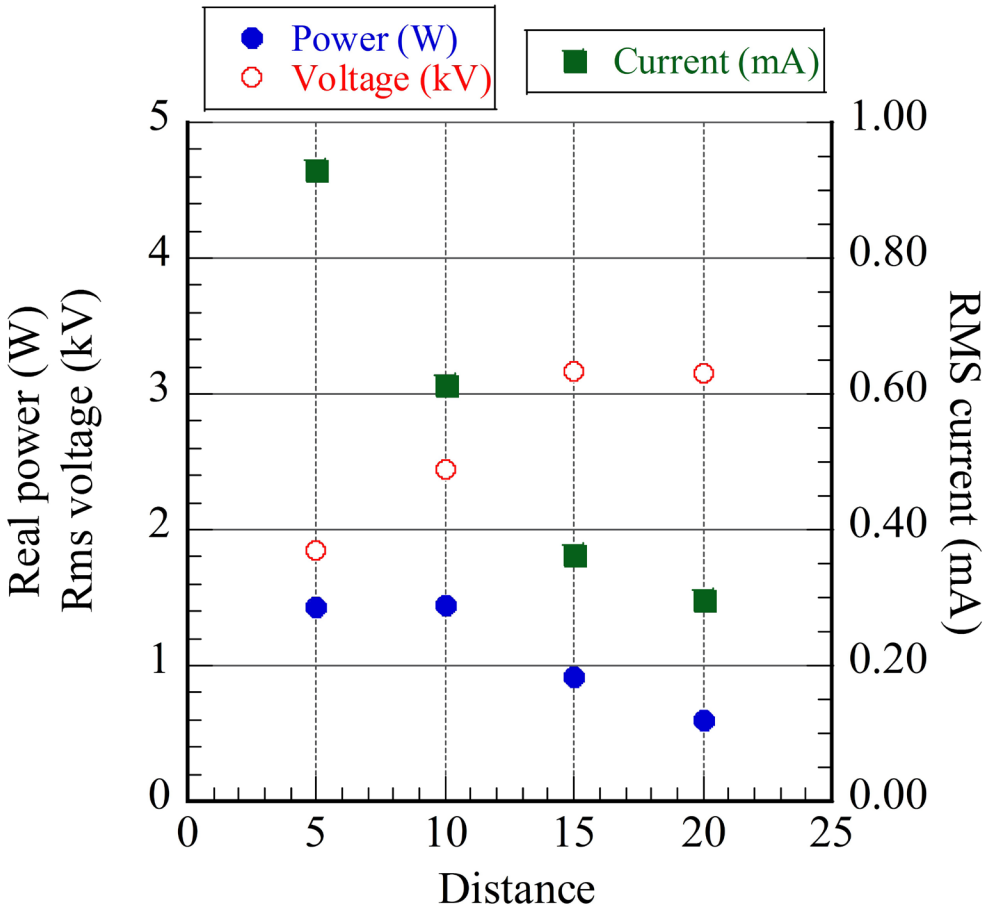

FIG. 6: RMS voltage (empty circle), RMS current (solid square), and real power (solid-circle) shown as functions of distance between the plasma exit of the LE-IGCE and the target plate

by cutting of the femoral artery of a C57BL6 mouse under anesthesia.[13,14] Fig. 8 shows a typical infrared thermo-image of the plasma-treated area. During treatment, the surface temperature remained at less than 40°C throughout (the power of the power supply was ~1 W, and the helium gas flow rate was 2.0 L/min.).

In the case of the HE-IGCE as shown in Fig. 4, Fig. 9 shows the time evolution of the high voltage applied to the discharge electrode, v(t), the current passing through the target plate, i(t), the real power, and the energy (time integrated real power) for a single pulse. Here, we adopt R_0 = 4 kΩ as the load resistance and RS = 50 Ω. The high-voltage pulses are applied every 50 ms. The distance between the electrode and the plate is 1 mm. The set power and the argon gas flow rate for 99.998% purity gas on the monitor of the controller were selected to be 15 W and 2.0 L/min, respectively.[23] As shown in

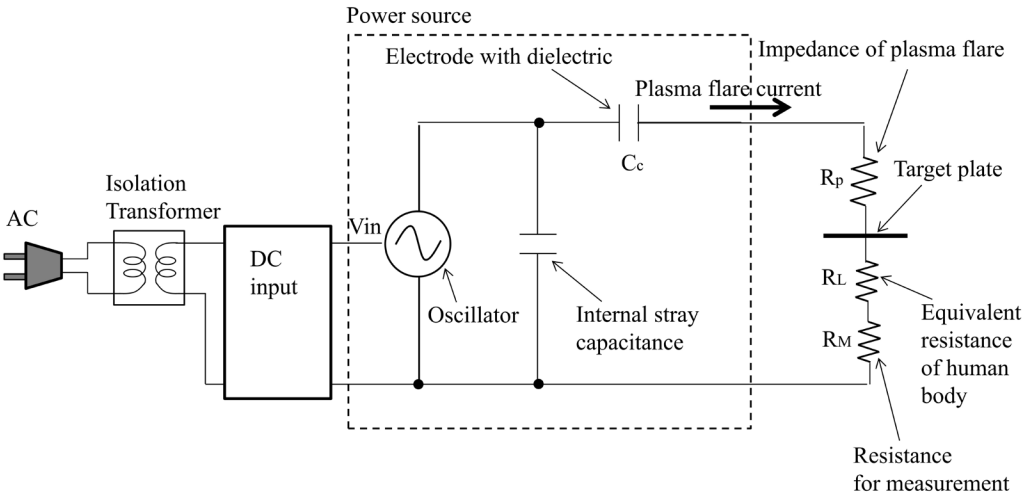

FIG. 7: Schematic diagram of electrical circuit used to study the power distribution for each impedance in the LE-IGCE

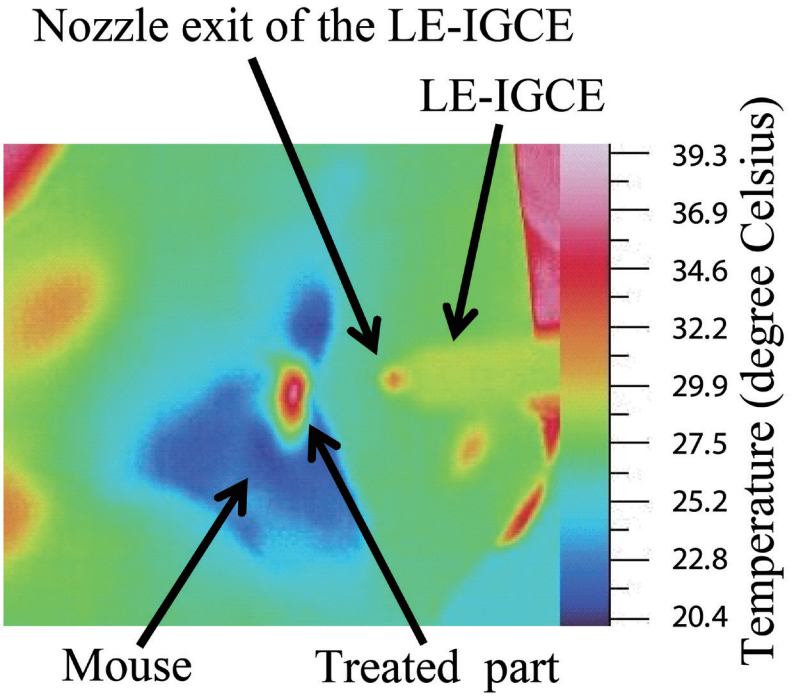

FIG. 8: Infrared thermo-image of the LE-IGCE plasma-treated area on the mouse

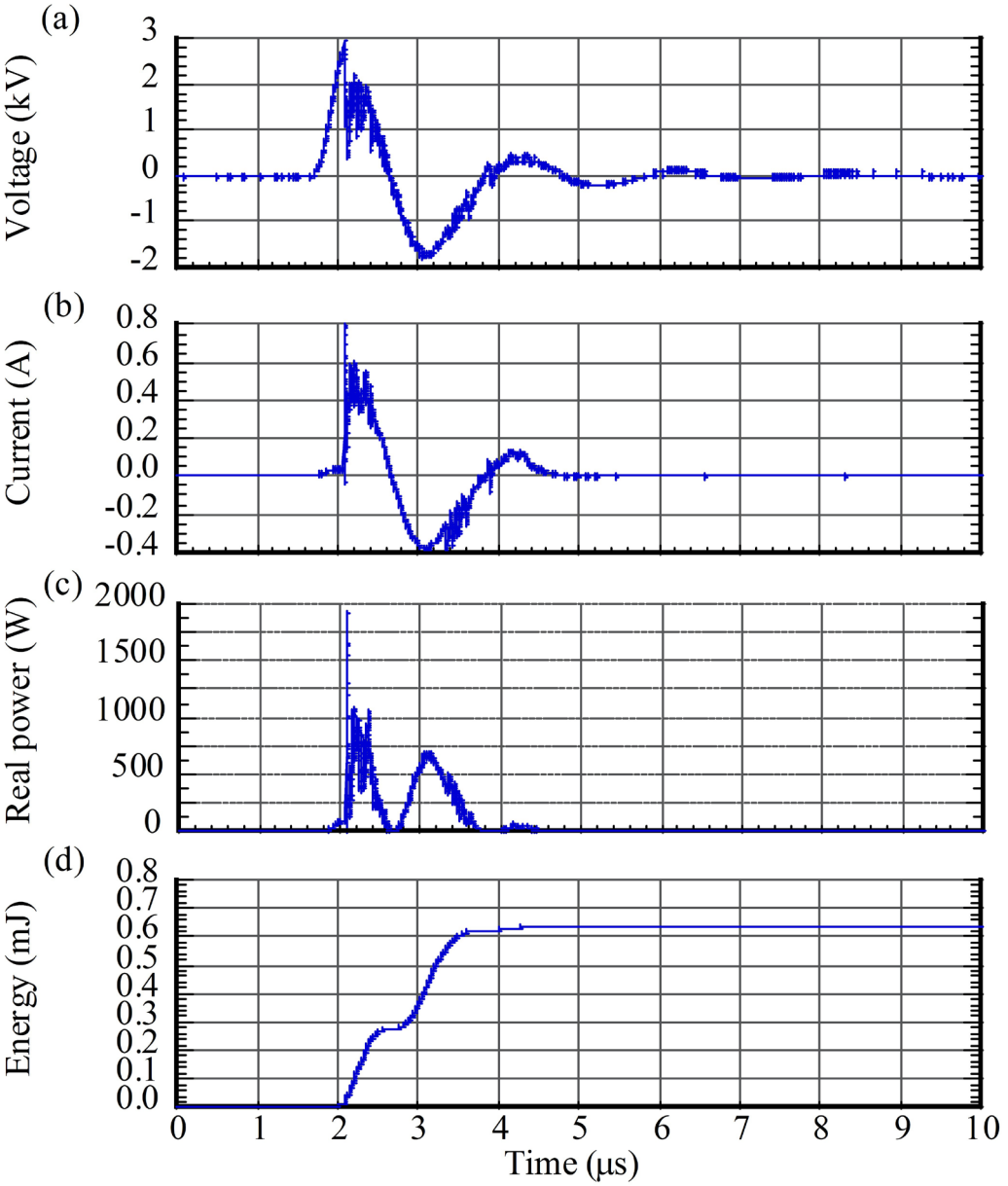

FIG. 9: Time evolutions of (a) high voltage applied to the discharge electrode, (b) the current passing through the target plate, (c) the real power, and (d) the energy (time integrated power)

Fig. 9(a) and (b), the voltage and current are in phase, which indicates an arc discharge. The real power is calculated using the data from Fig. 9(a) and (b), and is shown in Fig. 9(c). To estimate the energy per pulse, the real power from Fig. 9(c) is integrated for one

cycle, T(s), using equation (6) below, and gave a result of 0.64 mJ, as shown in Fig. 9(d).

(6) $E = \int_0^T v(t) \cdot i(t) dt$

Because the high-voltage pulses are applied every 50 ms, a total of 20,000 pulses are applied per second. The total energy for 1 s is estimated to be 0.64 (mJ) × 20,000 = 12.76 J. Therefore, the power for 1 s becomes 12.76 (J)/1 (s) ~ 12.8 W, which is close to the setting value.

Fig. 10 shows a schematic diagram of the assumed electric circuit used to study the power distribution for each impedance in the HE-IGCE. The internal impedance of the power supply, R_{in}, is assumed to be 1 kΩ. In the case where the arc voltage and the plasma peak current ($I_{P\text{-}peak}$) are 80 V and 1 A, respectively, the plasma resistance, R_p, is 80 Ω. $I_{P\text{-}peak}$ is calculated using equation (7).

(7) $I_{P\text{-}peak} = \frac{V_{peak}}{R_{in} + R_p + R_L + R_M} = \frac{4000\ \text{V}}{1000\ \Omega + R_p + R_L + R_M}$

The powers for each load, that is P_{plasma}, P_{RL}, and P_{RM}, are estimated using equation (8).

(8) $P_{plasma}, P_{RL}, P_{RM} = \frac{1}{2} I_{p-peak}^2 \times \frac{1}{3} \times \tau \times n \times (R_p, R_L, R_M)$

Here, 1/3 represents a correction factor for the attenuation waveform. τ is the pulse width shown in Fig. 9(b), or 1.5×10^{-6} s, and n is the number of pulses during a period of 1 s, or 20,000/s. In the case where R_p = 80 Ω, the equivalent resistance for the human body R_L = 4 kΩ, and the resistance for the leakage current measurement R_M = 50 Ω, $I_{P\text{-}peak}$, P_{plasma}, P_{RL}, and P_{RM} can be calculated as follows:

(9) $I_{p-peak} = \frac{4000}{1000 + 80 + 4000 + 50} = 0.78\ A_{peak}$

(10) $P_{plasma} = \frac{1}{2}(0.78)^2 \times \frac{1}{3} \times 1.5 \times 10^{-6} \times 20{,}000 \times 80 = 0.24\ W$

(11) $P_{RL} = \frac{1}{2}(0.78)^2 \times \frac{1}{3} \times 1.5 \times 10^{-6} \times 20{,}000 \times 4000 = 12.2\ W$

(12) $P_{RM} = \frac{1}{2}(0.78)^2 \times \frac{1}{3} \times 1.5 \times 10^{-6} \times 20{,}000 \times 50 = 0.15\ W$

Therefore, the total power becomes 0.24 + 12.2 + 0.15 = 12.6 W, which is very close to the measured value (12.8 W) shown in Fig. 9. Note here that both the plasma power and the R_M power are very small, but the power and voltage ($4 \times 10^3\ \Omega \times 1$ A = 4 kV) of the equivalent resistance for the human body are very large. The surface temperature of the material during the operation when using the HE-IGCE increases because of ohmic heating, as demonstrated by Kim et al.[25]

IV. SUMMARY

Clipping, ligation, and cauterization are used as basic methods to control bleeding from small or mid-sized arteries, whereas bleeding from small and capillary vessels is con-

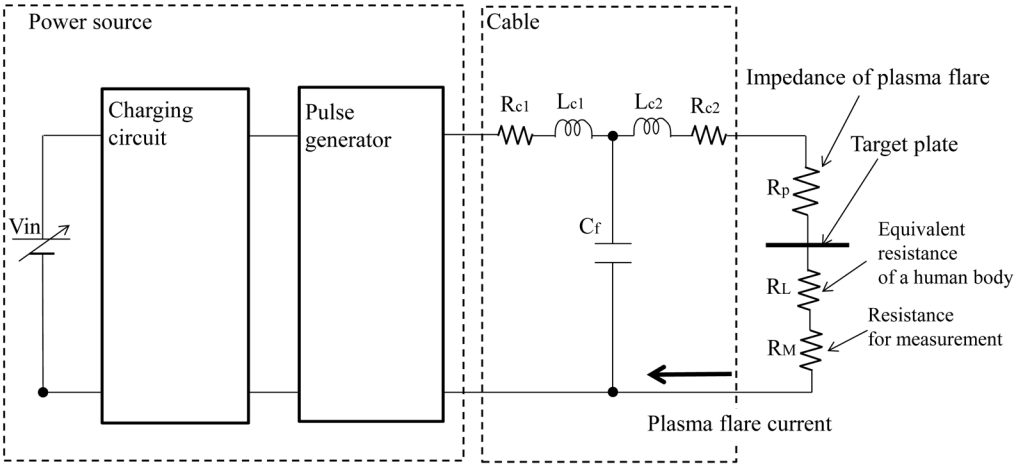

FIG. 10: Schematic diagram of the electrical circuit used to study the power distribution for each impedance in the HE-IGCE

trolled using the HFEC, ultrasonic wave equipment, lasers, and the HE-IGCE with the tissue damage. The scar tissues that result from burn injuries are characterized as a proliferation of fibroblast and blood vessels, called granulation tissue, and limits the performance of the second surgery. Blood coagulation using the LE-IGCE promptly covers the disrupted blood vessel and stops the bleeding with no evidence of burning or tissue damage. In this paper, to ensure the electrical safety of the LE-IGCE and the HE-IGCE, specifications such as the output current and the power of the equipment were measured and evaluated.

Based on the time evolution measurement of the voltage and the current in the LE-IGCE, the root mean square voltage, root mean square current, and the real power were calculated. Especially, the RMS current increases sharply as the distance between the exit of the plasma equipment and the target decreases. Moreover, because of the estimation of the power distribution for each impedance in the LE-IGCE circuit, the plasma resistance is ~1 MΩ, and ohmic heating caused by the plasma flare current in the human body is negligible (~2 mW). However, a part of energy that is used to produce the plasma flows into the human body (~3 W).

Based on the time evolution measurement of the voltage and current in the HE-IGCE, the power was calculated as ~12.8 W, which was close to the setting value. Moreover, from the estimation of the power distribution for each impedance in the HE-IGCE circuit, the plasma resistance was determined to be ~80 Ω. Both the plasma power and the R_M power are very small, but the power and voltage of the equivalent resistance for the human body are actually very high. The surface temperature of the material increases during the operation using the HE-IGCE because of ohmic heating.

We found that the power required to produce the plasma of the LE-IGCE corresponds to the real power of the power supply and is higher than that required for the

HE-IGCE. In addition, ohmic heating induced by the LE-IGCE in the human body is much less than that induced by the HE-IGCE.

ACKNOWLEDGMENTS

The authors would like to thank Dr. Susumu Makinouchi, Mr. Masaya Fujino, Mr. Shunji Watanabe, and Mr. Toru Imai at Nikon Corporation, and Mr. Masaaki Naito at AIST. This study was financially supported by the Strategic International Standardization Acceleration Projects and the R&D Guideline from the Ministry of Economy, Trade and Industry of Japan (METI), and in part by a Grant-in-Aid for Scientific Research on Priority Area (24108006) from the Ministry of Education, Culture, Sports, Science and Technology of Japan.

REFERENCES

1. Grund KE, Storek D, Farin G. Endoscopic argon plasma coagulation (APC) first clinical experiences in flexible endoscopy. Endoscope Surgery. 1994;2:42–6.
2. IEC 60601-2-2: 2009, Medical electrical equipment—Part 2-2: Particular requirements for the basic safety and essential performance of high frequency surgical equipment and high frequency surgical accessories.
3. Kanazawa S, Kogoma M, Moriwaki T, Okazaki S. Stable glow plasma at atmospheric pressure. J Phys D: Appl Phys. 1988;21(5):838–40.
4. Stoffels E, Flikweert AJ, Stoffels WW, Kroesen GMW. Plasma needle: a non–destructive atmospheric plasma source for fine surface treatment of (bio) materials. Plasma Sources Sci. T 2002;4:383–8.
5. Teschke M, Kedzierski J, Finantu-Dinu EG, Korzec D, Engemann J. High-speed photographs of a dielectric barrier atmospheric pressure plasma jet. IEEE Trans Plasma Sci. 2015;33:310–1.
6. Laroussi M, Lu X. Room temperature atmospheric pressure plasma plume for biomedical applications. Appl Phys Lett. 2005;87:113902.
7. Heinline J, Morfill G, Landthaler M, Stolz W, Isbary G, Zimmermann JL, Shimizu T, Karrer S. Plasma medicine: possible applications in dermatology. J Dtsch Dermatol Ges. 2010;8:968–76.
8. Park GY, Park SJ, Choi MY, Koo IG, Byun JH, Hong JW, Sim JY, Collins GJ, Lee JK. Atmospheric-pressure plasma sources for biomedical applications. Plasma Sources Sci Technol. 2012;21:043001.
9. Fridman G, Peddinghaus M, Ayan H, Fridman A, Balasubramanian M, Gutsol A, Brooks A, Friedman G. Blood coagulation and living tissue sterilization by floating-electrode dielectric barrier discharge in air. Plasma Chem Plasma Process. 2006;26:425–42.
10. Kuo SP, Chen CY, Lin CS, Chiang SH. Wound bleeding control by low temperature air plasma. IEEE Trans Plasma Sci. 2010;38:1908–14.
11. Kuo SP. Air plasma for medical applications. J Biomed Sci Eng. 2012;5(4):81–95.
12. Choi J, Mohamed AAH, Kang SK, Woo KC, Kim KT, Lee JK. 900-MHz nonthermal atmospheric pressure plasma jet for biomedical applications. Plasma Process Polym. 2010;7(2):58–63.

13. Sakakita H, Ikehara Y. Irradiation experiments on a mouse using a mild-plasma generator for medical applications. J Plasma Fusion Res. 2010;5:S2117.
14. Ikehara Y, Sakakita H, Shimizu N, Ikehara S, Nakanishi H. Formation of membrane-like structures in clotted blood by mild plasma treatment during hemostasis. J Photopolym Sci Technol. 2013;26(4):555–7.
15. Yamada H, Yamagishi Y, Sakakita H, Tsunoda S, Kasahara J, Fujiwara M, Kato S, Itagaki H, Kim J, Kiyama S, Fujiwara Y, Ikehara Y, Ikehara S, Nakanishi H, Shimizu N. Turbulent enhancement and flow control of a neutral gas containing an atmospheric pressure plasma. Jpn J Appl Phys. 2016;55:01AB08.
16. Oh J, Walsh JL, Bradley JW. Plasma bullet current measurements in a free-stream helium capillary jet. Plasma Sources Sci Technol. 2012;21:034020.
17. Ito Y, Fukui Y, Urabe K, Sakai O, Tachibana K. Effect of series capacitance and accumulated charge on a substrate in a deposition process with an atmospheric-pressure plasma jet. Jpn J Appl Phys. 2010;49(6):066201.
18. IEC 60601-1: Medical electrical equipment - Part 1: General requirements for basic safety and essential performance.
19. IEC 60601-1-2: Medical electrical equipment - Part 1-2: General requirements for basic safety and essential performance - Collateral Standard: Electromagnetic disturbances - Requirements and tests.
20. ISO 14971: Medical devices -- Application of risk management to medical devices.
21. Sakakita H, Ikehara Y, Kiyama S. Plasma irradiation treatment device. WO2012/005132.
22. Sakakita H, Ikehara Y, Kiyama S. Plasma evaluation apparatus. WO 2013077126 A1.
23. http://www.erbe-med.com/globalHome/index.php.
24. Fujiwara Y, Sakakita H, Yamada H, Yamagishi Y, Itagaki H, Kiyama S, Fujiwara M, Ikehara Y, Kim J. Observations of multiple stationary striation phenomena in an atmospheric pressure neon plasma jet. Jpn J Appl Phys. 2016;55:010301.
25. Kim J, Sakakita H, Yamada H, Ikehara S, Nakanishi H, Niwa T, Shimizu N, Ichinose M, Ikehara Y. Study on thermal characteristics of the ionized gas coagulation equipment. Plasma Med. 2015;5(2):99–108.